Supertransferred Hyperfine Fields at ^{7}Li: Variable Temperature ^{7}Li NMR Studies of $LiMn_2O_4$-Based Spinels

Becky Gee,† Craig R. Horne, Elton J. Cairns, and Jeffrey A. Reimer*

Environmental Energy Technologies Division, Lawrence Berkeley Laboratory, and Departments of Chemical Engineering and Materials Science and Mineral Engineering, University of California at Berkeley, Berkeley, California 94720-1462

Received: May 19, 1998; In Final Form: August 18, 1998

The temperature dependence of the ^{7}Li NMR shift was measured for $LiMn_2O_4$, $LiMn_{2-y}Ni_yO_4$ ($y = 0.1$, 0.25, 0.33), $LiMn_{2-y}Co_yO_4$ ($y = 0.25$, 0.5, 1.0), $Li[Mn_{2-y}Li_y]O_4$ ($y = 0.1$, 0.33), and λ-MnO_2 spinel oxides. The ^{7}Li NMR shift can be separated into temperature-independent and -dependent components. The temperature-dependent shift follows the Curie−Weiss behavior of the bulk magnetic susceptibility. The temperature-independent shift is attributed to contributions from van Vleck and diamagnetic susceptibilities. Pauli susceptibility may also contribute to the temperature-independent shift in the nickel- and cobalt-substituted spinels. Supertransferred hyperfine (STH) coupling constants were derived from the ^{7}Li NMR shifts and bulk magnetic susceptibility data. The progressive increase in average nominal manganese oxidation state from +3.5 to +4 results in an increase in the supertransferred hyperfine field at the ^{7}Li nucleus in the lithium-substituted samples. Replacement of manganese by either cobalt or nickel also results in a larger STH field at the ^{7}Li nuclei. The increase in STH field for the lithium-, nickel-, and cobalt-substituted spinel oxides may arise from a greater covalence in these materials relative to the parent $LiMn_2O_4$ spinel oxide.

Introduction

Mixed ionically and electronically conducting transition-metal spinel oxides have been studied extensively because of their potential use as the electrode material in lithium secondary batteries. In particular, the cubic $LiMn_2O_4$ spinel has been studied for its potential use as the cathode material in lithium secondary batteries due to its low cost and toxicity.[1,2] Unfortunately, repeated cycling of $LiMn_2O_4$ in the 3V region (vs Li/Li^+), i.e., insertion and extraction of Li^+ into $LiMn_2O_4$, results in a substantial capacity fade. This large capacity fade has been attributed to a cubic-to-tetragonal (c/a = 1.16) distortion associated with the cooperative Jahn−Teller effect at the Mn^{3+} cations. Degradation of the electrode particles at crystallite surfaces is then viewed as being caused by the large lattice mismatch between bulk cubic $LiMn_2O_4$ and surface tetragonal $Li_2Mn_2O_4$; bulk volume expansion and contraction is also possible.[2,3] Whether surface or bulk, however, this volume change renders the $LiMn_2O_4$ spinel unsuitable for use in rechargeable lithium cells.

The search for materials that exhibit superior cycling performance to $LiMn_2O_4$ has led to the study of transition-metal- and cation-substituted materials isostructural to $LiMn_2O_4$. Substitution of Mn by cations such as Ni, Li, Cr, and Al is believed to enhance the cycling stability of the electrode material.[4−6] Nickel-substituted $LiMn_{2-y}Ni_yO_4$ has exhibited stable capacities on cycling, although nickel substitution results in a lower initial capacity due to the reduction in Mn^{3+} content,[5,7,8] A recent powder X-ray diffraction study shows formation of a tetragonal $Li_2Mn_2O_4$ spinel upon Li^+ insertion into $LiMn_2O_4$, whereas on insertion of Li^+ into $LiMn_{1.5}Ni_{0.5}O_4$ to form $Li_2Mn_{1.5}Ni_{0.5}O_4$ the spinel remains cubic.[8]

The electronic structure of spinel oxides is also a sensitive probe of Jahn−Teller effects. Overlapping transition metal d states may produce wide or narrow band structures with concomitant metallic properties; electrostatic repulsions, however, tend to keep d-state electrons localized on individual atoms, resulting in paramagnetic, insulating materials with unpaired electrons occupying discrete molecular orbitals. Thus, a transition from metallic to insulating behavior may occur through a change in composition and average oxidation state of the transition-metal ion. For example, the electronic properties of $La_{1-x}Sr_xMnO_3$ ($0 \le x \le 1$) perovskites are composition-dependent. Electron repulsion localizes the d-state electrons in both $LaMnO_3$ and $SrMnO_3$, rendering them nonmetallic; $LaMnO_3$ exhibits a cooperative Jahn−Teller distortion originating at the Mn^{3+} ions. Replacement of lanthanum by strontium in the perovskite lattice results in the formation of Mn^{4+} ions (in order to maintain charge balance); the cooperative Jahn−Teller distortion is no longer present, and metallic conductivity is found when approximately $x \ge 0.1$ due to delocalization of the electrons in the e_g band.[9]

We surmise that covalent or metallic bonding may play a significant role in suppressing the Jahn−Teller deformation when Li^+ is inserted into the spinel lattice of substituted materials. The reported absence of the tetragonal transformation in $LiMn_{1.5}Ni_{0.5}O_4$ and stable electrochemical cycling behavior may be due to an increase in the Mn^{4+} concentration as the nickel substituent level increases. Electrochemical insertion of Li^+ into $LiMe_{0.04}Mn_{1.96}O_4$ (Me = Co or Ni) supresses the severity of the Jahn−Teller effect although over 50% of the B sites remain occupied by Mn^{3+}.[43] Covalent effects arising from the substituent transition metal ion and the presence of greater Mn^{4+} concentrations may play an important role in suppressing the tetragonal phase change. In light of this hypothesis, we believe that characterization of the NMR properties of nuclei

* Corresponding author.
† Current address: Department of Chemistry, Long Island University, Brooklyn, NY 11201.

10.1021/jp982301p CCC: $15.00
Published on Web 11/19/1998

such as ^{7}Li will be useful in assessing the electronic structure of the spinel oxide materials.

Previous nuclear magnetic resonance (NMR) spectroscopy studies have offered some preliminary insight into the origin and interpretation of the ^{7}Li NMR shifts in $LiMn_2O_4$. The ^{7}Li NMR shift of $LiMn_2O_4$, with respect to an aqueous solution of LiCl, at a single temperature was assigned to a Knight shift, thereby attributing a metallic character to $LiMn_2O_4$. Based on this assignment, a density of states nearly equal to one, and therefore an apparent valence state of zero was assigned to the lithium.[10,11]

Much of the subsequent literature has attributed the observed ^{7}Li shifts to an interaction of localized d-state unpaired electrons with the ^{7}Li nucleus. Lithium-7 MAS (magic angle spinning) NMR results at ambient temperature were interpreted in terms of a transferred hyperfine interaction between lithium nuclei and localized d electron moments of the manganese cations which follow a Curie Law dependence.[12] A ^{7}Li and ^{6}Li MAS NMR study at ambient temperature of $LiMn_2O_4$ did not explicitly interpret the source of the isotropic shifts but did assert the unlikelihood of a Knight shift.[13] Qualitative interpretation of temperature-dependent ^{7}Li NMR data attributes the resonance shifts and line widths to interactions between electron spins localized on manganese ions and the ^{7}Li nuclei.[14] Other work has correlated the temperature dependence of the measured paramagnetic susceptibility with the ^{7}Li resonance shifts and line widths for oxygen-deficient $LiMn_2O_{4-\delta}$ spinels.[15] Magnetic ordering of the electronic moments in $LiMn_2O_4$ was also examined by bulk susceptibility and variable temperature ^{7}Li NMR experiments.[16]

The present work addresses degree of covalence in $LiMn_2O_4$-based spinels by determination of ^{7}Li transferred hyperfine coupling constants through variable temperature solid-state ^{7}Li NMR and bulk magnetic susceptibility measurements. We find that the progressive increase in average nominal manganese oxidation state from +3.5 to +4 results in an increase in the supertransferred hyperfine field (STHF) at the ^{7}Li nucleus in lithium-substituted samples. Replacement of manganese by either cobalt or nickel also results in a larger STHF at ^{7}Li nuclei in these spinel oxides. The increase in STHF for the substituted samples may arise from a greater covalence in these materials relative to the parent $LiMn_2O_4$ spinel oxide.

Experimental Section

Sample Preparation and Characterization. Samples of $LiMn_2O_4$, $LiMn_{2-y}Ni_yO_4$ ($y = 0.1, 0.25$), $LiMn_{2-y}Co_yO_4$ ($y = 0.25, 0.5$), and $LiMn_{2-y}Li_yO_4$ ($y = 0.1$) were prepared by grinding and mixing together stoichiometric amounts of MnO_2 (CMD, Japan Metals and Chemicals, IC#5), $LiOH{\cdot}H_2O$ (Spectrum Chemical, 99.9% purity), and $NiCO_3$ (Alfa-AESAR, 99% purity) or $CoCO_3$ (JT Baker) in *n*-hexane. The samples were subsequently transferred to a preconditioned alumina boat and heated at 20 °C/min to 750 °C for 40 h. The samples were then furnace cooled, reground in *n*-hexane, heated at 20 °C/min to 750 °C for 40 h, and cooled at 0.8 °C/min to 100 °C. Finally, the samples were furnace cooled to room temperature and reground in *n*-hexane.

The $LiMn_{1.67}Ni_{0.33}O_4$ and $LiMnCoO_4$ samples were prepared from $MnCO_3$ (JT Baker), Li_2CO_3 (JT Baker), and either $NiCO_3$ (Alfa Aesar) or $CoCO_3$ (JT Baker) powders. Each sample was mill mixed in acetone overnight and heated at 10 °C/min to 750 °C for 24 h, furnace cooled to room temperature, and reground. The samples were subsequently heated at 10 °C/min to 750 °C for 32 h, cooled at 0.8 °C/min to 100 °C, and allowed to furnace cool to room temperature.

$Li_4Mn_5O_{12}$ spinel was prepared by grinding stoichiometric amounts of Li_2CO_3 and $MnCO_3$. The resulting mixture was first heated at 350 °C for 44 h under flowing O_2 and then heated at 400 °C for an additional 24 h.

Chemical delithiation of $LiMn_2O_4$ to produce λ-MnO_2 was done by acid extraction. Three grams of $LiMn_2O_4$ was constantly stirred in 80 mL of 1 M H_2SO_4 for 26 h. The material was then dried overnight under vacuum at 80 °C.

The structures of all samples were confirmed by X-ray powder diffraction measurements. The nickel-substituted samples show relatively minor impurity phases which are estimated to constitute no more than 2 wt %. Soft X-ray absorption spectroscopy (SXAS) results at the transition metal $L_{II,III}$-edge show that in $LiMn_{1.75}Me_{0.25}O_4$ (Me = Ni or Co), nickel is present in the +2 oxidation state and cobalt is low spin and present in the +3 oxidation state.[17]

Bulk Magnetic Susceptibility Measurements. Field- and temperature-dependent magnetic susceptibility measurements were performed between 10 and 350 K on a Quantum Designs MPMS SQUID magnetometer. Powdered samples were carefully weighed and packed in polychlorotrifluoroethylene (Kel-F) sample holders. Corrections for the diamagnetic contribution from the Kel-F sample holders were made by measurement of the field dependent magnetic moment of the empty sample holders.

Solid-State NMR Spectroscopy. Solid-state ^{7}Li NMR experiments were performed using a home-built variable temperature probe and spectrometer operating at 70.35−70.39 MHz. A solid echo pulse sequence, $\theta_x - \tau - \theta_y$−acquire, with a 16-step phase cycle, was used to acquire the spectra.[18] Typical pulse lengths were $\theta_x = \theta_y = 1-2$ μs, while recycle delays of 700 ms to 1 s were sufficient to avoid saturation of the signal. All measurements were executed with 1 μs dwell times and echo delays of 40−60 μs. Each time domain signal was left-shifted to the echo maximum, convoluted with a Gaussian broadening function, and Fourier transformed to yield the frequency domain spectrum. A nonlinear regression routine in the Mathematica software application was used to fit the ^{7}Li resonances to Gaussian functions. All shifts are presented relative to 1 M LiCl(aq).

Results

Shown in Figure 1 are representative plots of the magnetization as a function of applied magnetic field strength at 350 K for a number of the spinel oxide samples studied. The linear and reversible dependence of the bulk magnetization on the applied magnetic field strength, the positive slope, and the extrapolated value of zero magnetization in the absence of an applied field indicate that these spinel oxides are paramagnetic at 350 K. A minor remnant magnetization is present in all the nickel samples studied. This may arise from the impurity phase(s) detected by powder X-ray diffraction work. The reciprocal value of the magnetic susceptibility as a function of temperature is presented in Figure 2. All samples follow the Curie−Weiss law at temperatures above 150−250 K. The Weiss constants determined by extrapolation of the data to $\chi^{-1} = 0$ in the appropriate temperature range are presented in Table 1. The Weiss constants for $LiMn_2O_4$, λ-MnO_2, and $Li_4Mn_5O_{12}$ are in good agreement with those presented in the literature.[4,19,20]

Estimated values of diamagnetic and van Vleck susceptibilities are nearly the same magnitude yet opposite in sign. The van Vleck and diamagnetic susceptibilites for $LiMn_2O_4$ are $\chi = +5 \times 10^{-9}$ m^3/kg and $\chi = -5 \times 10^{-9}$ m^3/kg, respectively. Corrections for the sample diamagnetism and van Vleck

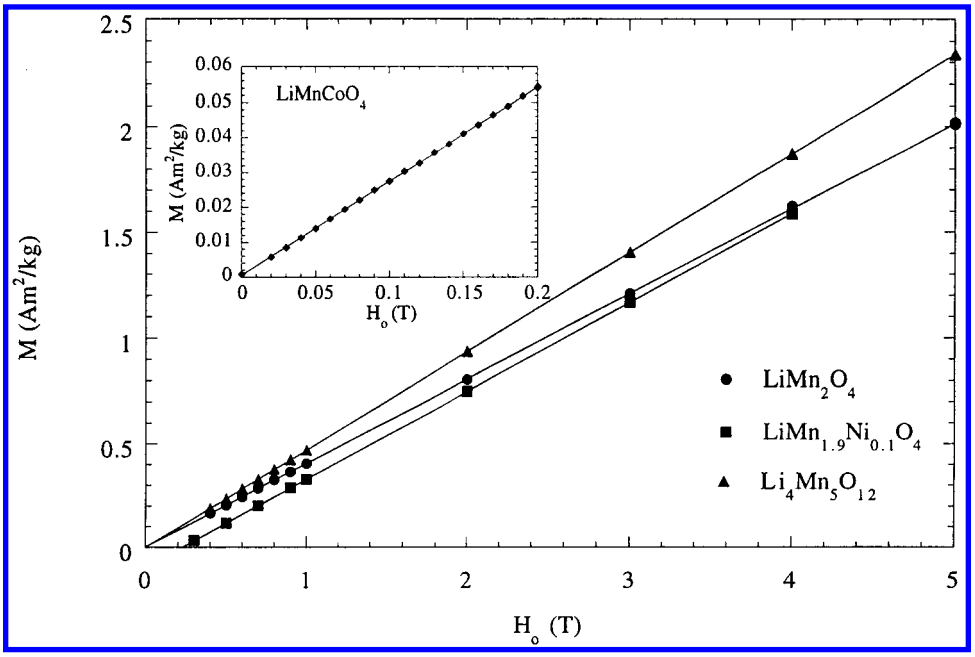

Figure 1. Magnetization as a function of applied magnetic field at 350 K for representative spinel oxide samples studied.

paramagnetism were therefore not made, since these contributions nearly cancel. However, these effects may still contribute to the temperature-independent component of the ^{7}Li NMR shifts (see Discussion section).

Previous studies of $LiMn_2O_4$ have shown the existence of a low-temperature cubic to tetragonal (c/a = 1.01) phase transformation at approximately 280 K due to the cooperative Jahn−Teller effect originating at the Mn^{3+} cations.[4,21] However, a least-squares fit to the inverse of the susceptibility data below the reported phase transition temperature region to that above produced no significant difference in the calculated Weiss and Curie constants.

The static ^{7}Li NMR spectra of $LiMn_2O_4$ are shown as a function of temperature with their respective least-squares fits in Figure 3. The ^{7}Li resonance shifts and line widths for the spinel oxides in this work are notably larger than those found in diamagnetic solids, suggesting a significant interaction among the ^{7}Li nuclei and unpaired electrons. Typical ^{7}Li resonance shifts are in the range of +20 to −30 ppm (vs 1 M LiCl(aq)) due to the high electropositive character of lithium,[22] whereas the ^{7}Li line widths of the central transition in diamagnetic solids are on the order of a few kilohertz (fwhm) and can be often attributed to strong dipolar interactions among ^{7}Li nuclei.

As the temperature is increased, the ^{7}Li shift and fwhm for the $LiMn_2O_4$ spinel steadily decreases in agreement with data published previously.[14,15] At all temperatures, the line shape is excellently fit by a single Gaussian function. The ^{7}Li NMR spectra of all other spinel samples examined are also single broad Gaussians, with shifts at 294 K in the range 495−940 ppm with respect to an aqueous solution of 1 M LiCl(aq). These data are shown in Figure 4.

Discussion

The Origin of NMR Shifts. The presence of unpaired electrons in solids markedly affects the NMR resonance shift and line width due to couplings among the electronic and nuclear moments. Generally, the coupling may consist of a dipolar interaction between nuclei and non-s-state unpaired electrons and a hyperfine coupling between s-state unpaired electrons and nuclei.

The dipolar interactions among unpaired electrons in states with nonzero orbital angular momentum and magnetic nuclei give rise to line broadening. The extent of the broadening is determined by the proximities of the unpaired electrons to the nuclei of interest and the nuclear and thermally averaged electronic magnetic moments. A pseudocontact shift may also be present for paramagnetic ions in noncubic environments due to the coupling of the orientationally dependent electron orbital angular momentum (anisotropic **g**-tensor) and the spin angular momentum.[23]

The dipole approximation is no longer valid for unpaired electrons with s-state character wave functions. In this situation the coupling between unpaired electrons and nuclei is generally described by a hyperfine interaction that depends on the degree of unpaired spin density at the nucleus of interest. In the most general form this interaction gives rise to a shift described by

$$\delta = \frac{\Delta\omega}{\omega_0} = -\frac{A}{\omega_0\hbar}\langle S_z\rangle \tag{1}$$

where $\Delta\omega$ is the shift of the resonance frequency relative to a standard, ω_0 is the Larmor frequency of the nucleus, and A is the hyperfine coupling constant, which is a measure of the unpaired electron spin density present at the nucleus of interest. The time-averaged value of the electron spin $\langle S_z\rangle$ is proportional to the magnetic molar susceptibility χ (m^3/mol) of the unpaired electrons and is expressed as[24,25]

$$\chi_{mol} = -\frac{\mu_0 g N_o \mu_B}{H_o}\langle S_z\rangle \tag{2}$$

where g is the electron g factor, H_0 is the applied static magnetic field, N_o is Avogadro's number, μ_0 is the permeability, and μ_B is the Bohr magneton. The shift can then be expressed as

$$\delta = B\chi_{mol} \tag{3}$$

where $B = A/(\gamma\hbar g\mu_B N_o\mu_0)$ and γ is the nuclear gyromagnetic ratio of the nucleus of interest.

In paramagnetic compounds there are a number of possible contributions to the isotropic NMR shift. Diamagnetic, van

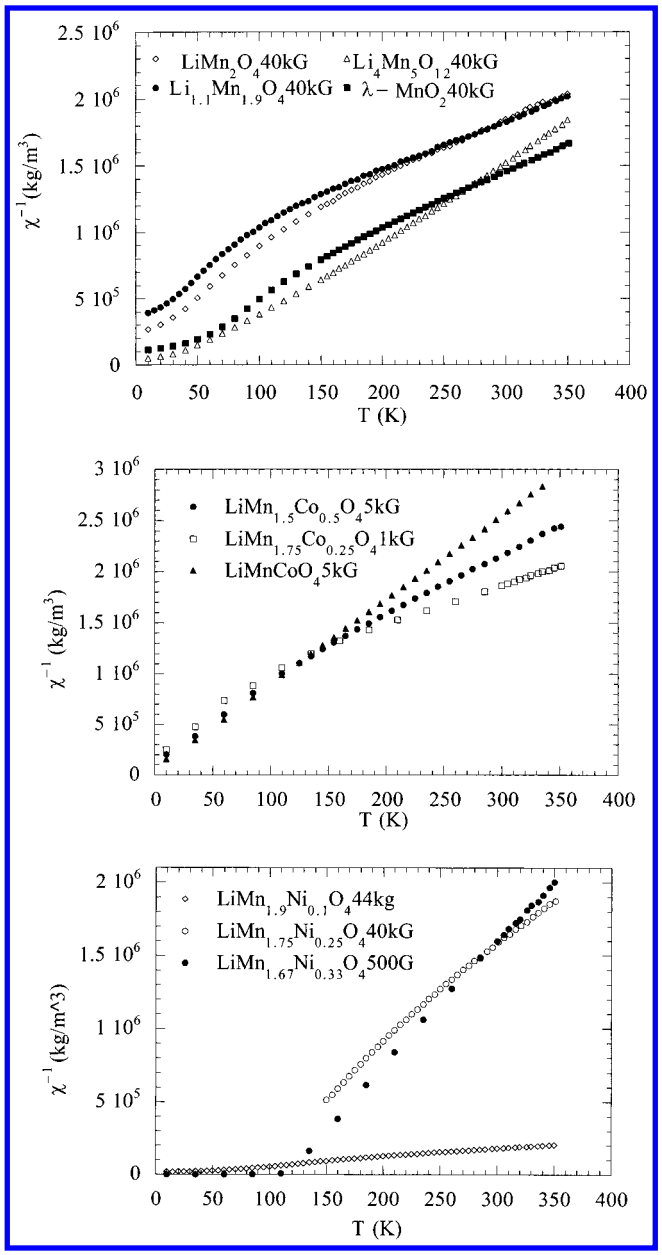

Figure 2. Reciprocal value of the magnetic susceptibility as a function of temperature (field strengths are noted in the figure). The determined Weiss constants are reported in Table 1.

TABLE 1: Bulk Magnetic Susceptibility and ^{7}Li NMR Parameters for Oxide Spinels[a]

nominal composition	Weiss const (K)	transferred hyperfine coupling const, 10^6 rad/s
$LiMn_2O_4$	−231	8.6 ± 0.4
		8.6 ± 0.3
$Li_{1.1}Mn_{1.9}O_4$	−148	9.3 ± 0.3
$Li_4Mn_5O_{12}$	48	10.9 ± 0.4
$LiMn_{1.9}Ni_{0.1}O_4$	−48	9.8 ± 0.3
$LiMn_{1.75}Ni_{0.25}O_4$	36	10.0 ± 0.2
$LiMn_{1.67}Ni_{0.33}O_4$	113	13.4 ± 0.2
$LiMn_{1.75}Co_{0.25}O_4$	−197	9.6 ± 0.4
$LiMn_{1.5}Co_{0.5}O_4$	−70	11.8 ± 0.5
$LiMnCoO_4$	−9	13.8 ± 0.5
λ-MnO_2	−55	11.6 ± 0.6

[a] Two independent sets of ^{7}Li NMR were used to determine the transferred hyperfine coupling constant for the $LiMn_2O_4$ spinel. Good reproducibility was obtained.

Vleck, Pauli, and Curie−Weiss susceptibilities may contribute to the resonance shift. The isotropic resonance shift can be written as sum of all components

$$\delta = \Delta\omega/\omega_o = B_{cw}\chi_{cw} + (B_{vv}\chi_{vv} + B_p\chi_p + \delta_{dia}) \quad (4)$$

where the $B_{cw}\chi_{cw}$ term is due to coupling of nuclei with unpaired electrons that obey the Curie−Weiss law. The second and third terms are associated with van Vleck and Pauli paramagnetisms, respectively, and the last term, δ_{dia}, is the diamagnetic shift. Both van Vleck and diamagnetic susceptibilities are temperature-independent, and their possible contributions to the ^{7}Li NMR shift will be addressed later in the Discussion section.

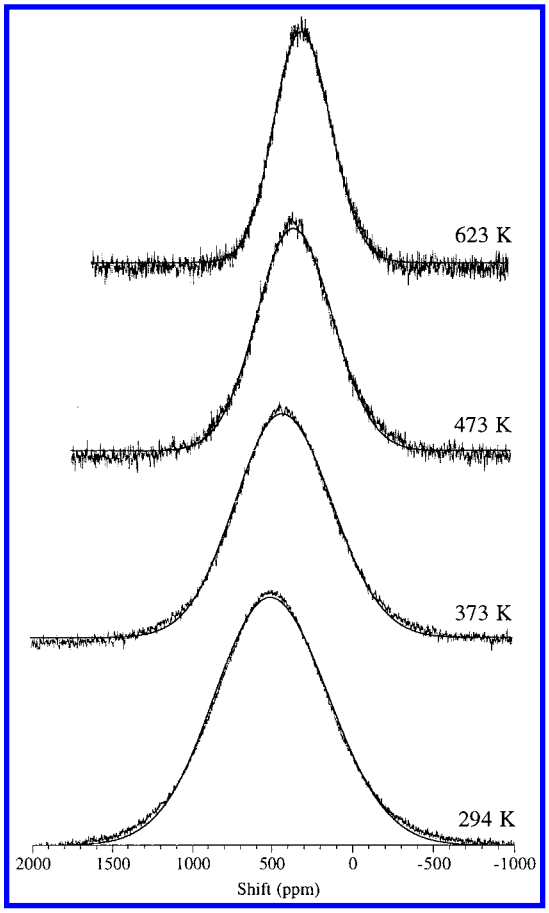

Figure 3. Representative static ^{7}Li NMR spectra of $LiMn_2O_4$ are shown as a function of temperature with their respective least-squares fits. All intensities are arbitrarily scaled.

Pauli paramagnetism is exhibited by metallically conducting materials and may give rise to a temperature-independent NMR shift known as the Knight shift. Only those electrons near the Fermi level are allowed to align parallel to the applied magnetic field due to the absence of available unoccupied states close in energy. Thermal fluctuations of the electronic spin states near the Fermi level are quenched due to the unavailability of empty states. The NMR shift in metals is therefore generally expected to be independent of temperature and positive for direct interaction of the Pauli spin density and the nucleus of interest.

In contrast, the magnetic susceptibility of localized electrons closely follows an inverse temperature dependence due to thermal agitation of the spin moments. The magnetic molar susceptibility of localized moments will exhibit Curie−Weiss behavior in the absence of strong ferromagnetic, ferrimagnetic, or antiferromagnetic couplings and is described by

$$\chi_{cw} = C/(T - \theta) \quad (5)$$

where C is the Curie constant, $C = (\mu_0 N_0 \mu_{eff}^2/3k)$, μ_0 is the

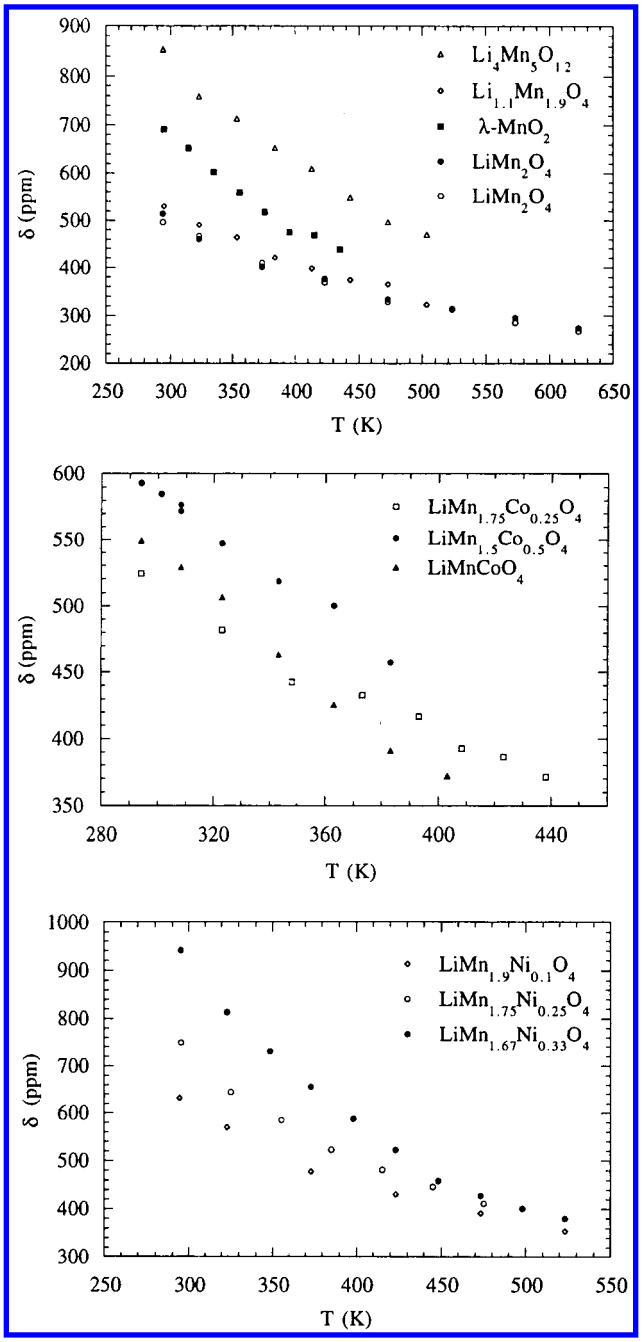

Figure 4. Temperature dependence of the ^{7}Li NMR shift for all spinel oxides studied.

permeability, N_0 is Avogadro's number, and μ_{eff} is the effective number of Bohr magnetons per moment. The Weiss constant, θ, typically accounts for magnetic ordering of the electronic moments below the Curie or Néel temperatures. Possible deviations from the Curie law, $\chi = C/T$ due to van Vleck paramagnetism may also appreciably affect the measured Weiss constant for 3*d* transition-metal compounds. Thus, the absolute value of the experimentally measured Weiss constant does not necessarily reflect the Curie or Néel ordering temperature for the electronic moments.

Due to the difference in temperature dependencies of the magnetic susceptibilities of localized and delocalized electrons, temperature-dependent studies of the NMR shift may be used to deconvolute the temperature-dependent and -independent components of the resonance shift. Extrapolation of the NMR shift as a function of $1/(T - \theta)$ to infinite temperature provides a measure of the temperature-independent components of the

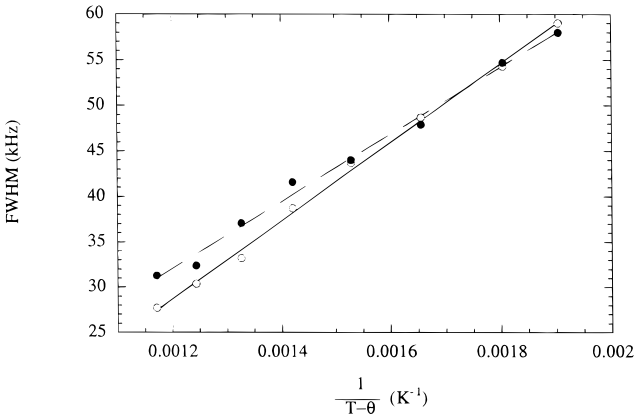

Figure 5. Full width at half-maximum (fwhm) of the ^{7}Li resonance as a function of $1/(T - \theta)$ for $LiMn_2O_4$. The two data sets acquired for the same sample of $LiMn_2O_4$ are presented.

shift and in some cases can furnish information concerning the extent of electron delocalization in systems containing both localized and delocalized electrons. This approach has been successfully demonstrated by high-temperature ^{17}O NMR measurements of transition-metal perovskites.[26] The hyperfine interaction at the nucleus of interest can be obtained from the slope of the NMR shift versus $1/(T - \theta)$ plot, thereby providing a measure of the unpaired electron spin density at the nucleus.

Large magnetic hyperfine fields at diamagnetic cations have been observed in numerous systems. Magnetic hyperfine fields have been observed at diamagnetic A-site Cu^+ and Cd^{2+} cations in $Fe_{0.5}Cu_{0.5}Cr_2S_4$ and Cd-doped $Li_{0.4}Fe_{2.5}O_4$ spinels, respectively.[27,28] The hyperfine fields at these cations were attributed to the transfer of unpaired spin density from the magnetic cation via the interleaving oxygen ion to the nominally diamagnetic cation. This type of hyperfine field is known as the super-transferred hyperfine (STH) field.

The STH field depends on the covalency of the diamagnetic ion−oxygen and transition metal−oxygen bonds through overlap and electron-transfer effects.[29,30] Although the contributions to the STH field are difficult to predict theoretically, it is known that the magnitude of the STH field increases as the covalency of the diamagnetic cation−oxygen and/or transition metal−oxygen bonds increases.[30,31]

Analysis of the Present Data. The full width at half-maximum (fwhm) data of the ^{7}Li resonance for the $LiMn_2O_4$ spinel are presented as a function of $1/(T - \theta)$ in Figure 5. The fwhm nearly follows a linear dependence, suggesting that the exceedingly strong couplings among the ^{7}Li nuclei and unpaired electrons masks any potential information concerning the temperature dependence of the ^{7}Li mobility. Plots of the fwhm as a function of $1/(T - \theta)$ for all other spinel samples studied exhibit the same behavior.

A plot of the ^{7}Li NMR shift as a function of $1/(T - \theta)$ is presented in Figure 6 for $LiMn_2O_4$. All spinel oxides show a linear relationship between the ^{7}Li NMR shift and the bulk magnetic susceptibility. In contrast with the Knight shift of metallic lithium (270 ppm), the large values of the isotropic ^{7}Li NMR shift and their linear relationship to the Curie−Weiss behavior of the magnetic susceptibility suggest a paramagnetic shift due to hyperfine couplings of the nuclei with unpaired electron spin density. Extrapolation of the ^{7}Li NMR shift to infinite temperature shows a temperature-independent shift for all samples that is nearly independent of composition and average nominal manganese oxidation state (Figure 7). The slope of the ^{7}Li NMR shift versus $1/(T - \theta)$ data and the Curie

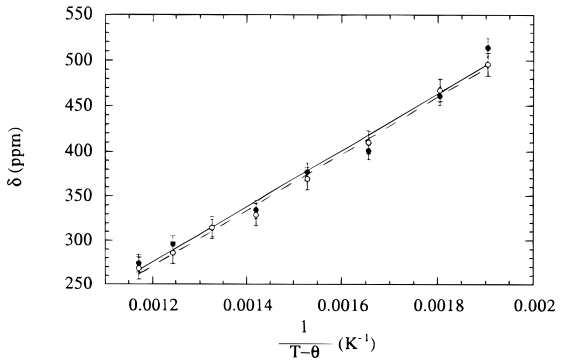

Figure 6. ^{7}Li NMR shift as a function of $1/(T-\theta)$. The two data sets acquired for the same sample of $LiMn_2O_4$ are presented. Good reproducibility for derived quantities such as the supertransferred hyperfine coupling constant (see Table 1) are obtained.

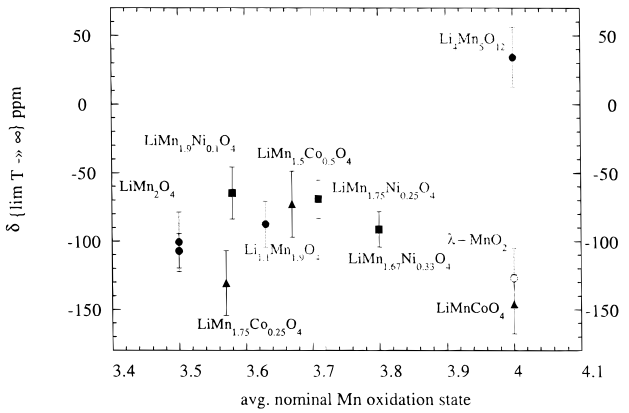

Figure 7. Temperature-independent component of the ^{7}Li NMR shift as a function of the average nominal manganese oxidation state.

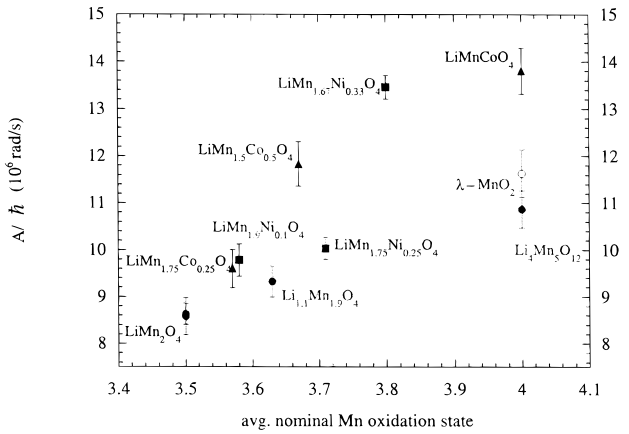

Figure 8. Supertransferred hyperfine coupling constants as a function of the average nominal Mn^{n+} oxidation state.

constant provide the ^{7}Li supertransferred hyperfine coupling constant for each sample. The STH coupling constants are presented in Table 1 and Figure 8 as a function of the average nominal Mn^{n+} oxidation state.

Temperature-Independent ^{7}Li NMR Shift. The temperature-independent component of the ^{7}Li NMR shift (Figure 7) may consist of contributions from diamagnetic and/or temperature-independent paramagnetic susceptibilities such as Pauli or van Vleck. The chemical shift in diamagnetic compounds can arise from the magnetic-field-induced spherical electron circulation of paired electrons and the field-induced nonspherical circulation of electron density which arises from the magnetic-field-induced mixing of ground and excited states. The temperature-independent van Vleck paramagnetism may also be present in compounds containing first-row transition-metal elements. This contribution to the magnetic susceptibility was first addressed by van Vleck in his second-order perturbation treatment of the Zeeman interaction.[32] The applied magnetic-field-induced mixing of excited d-state wave functions into the ground state gives rise to a magnetization. The van Vleck paramagnetic contribution to the total susceptibility is temperature-independent for excited states whose energies lie well above the ground state relative to the thermal energy (i.e., $E_{\text{exited}} - E_{\text{ground}} \gg kT$).[3] Transition-metal ions with A_{2g} (d^3 and d^8 in an O_h field) and E_g (d^4 in an O_h field) ground terms will exhibit van Vleck paramagnetism.[33]

Typical isotropic chemical shifts for $^7Li^+$ ions in solids range from −30 to +20 ppm with respect to 1 M LiCl(aq).[22] Both diamagnetic and van Vleck susceptibilities may certainly contribute to the temperature-independent ^{7}Li NMR shift in these spinels. However, with the exception of $Li_4Mn_5O_{12}$, the temperature-independent component of the ^{7}Li NMR shift in the compounds studied are outside of these limits.

Another origin of the temperature-independent shift may be the presence of Pauli paramagnetism. Knight shifts in metals are generally positive since the additional magnetic field at the nucleus produced by s-state electrons is parallel to the electron magnetic moment, and this electronic moment is preferentially aligned parallel to the applied static magnetic field. However, for d-state electrons the exchange interaction between the d-state electrons at the Fermi level and core s-state electrons results in polarization of inner-shell s-state electrons.[34] Electron spin density with s-state character interacts with the nucleus through contact or spin dipolar interactions. Core polarization by d-state electrons results in negative Knight shifts. The large negative shift (−320 ppm at 300 K) for the ^{7}Li nuclei in the layered intercalation compound Li_2VSe_2 was attributed to this mechanism.[35]

The $LiMn_2O_4$ spinel is a small polaron conductor. Direct interactions between the manganese d orbitals in $LiMn_2O_4$ are too weak to form a wide itinerant-electron bandwidth. This results in localized electrons in a t_{2g}^3 configuration and an electron in an e_g^1 configuration whose mobility is described by a thermally activated hopping between Mn^{3+} and Mn^{4+} sites often known as "small polaron" conduction.[36−38] The electronic moments in $LiMn_2O_4$ are expected to follow the Curie−Weiss law in the paramagnetic state.[19,36,39] The temperature-independent ^{7}Li NMR shift in $LiMn_2O_4$ may be attributed to diamagnetic and van Vleck susceptibilities. The presence of a finite 3d bandwidth may also give rise to a Knight shift contribution. It is difficult to assess quantitatively the exact contributions to the temperature-independent shift.

Diamagnetic and van Vleck susceptibilities may also contribute to the temperature-independent shift in the substituted spinel oxides, and they should solely give rise to the temperature-independent shift in $Li_4Mn_5O_{12}$. This spinel is an insulator due to the absence of any e_g electrons which are responsible for the electronic conduction in these materials. The observed temperature-independent shift, within experimental error, is within the limits observed for diamagnetic lithium-containing solids.

The Pauli susceptibility may contribute to the temperature-independent shift for those samples that are metallically conducting. Substitution of nickel, cobalt, or lithium for manganese may result in a contraction of the spinel lattice, leading to metallic conductivity which would give rise to Pauli paramagnetism. Therefore, it is certainly possible that electron

delocalization in the e_g band may contribute to the temperature-independent ^{7}Li NMR shift in the substituted spinel oxides. Further studies correlating conductive behavior through Seebeck coefficient measurements with the temperature-independent shift may be helpful. Spin−lattice relaxation studies may also prove useful, although the presence of localized d-state electrons may complicate interpretation of the data.

Supertransferred Hyperfine Interaction at the ^{7}Li Nucleus. Direct delocalization of the unpaired transition-metal d-electrons to lithium s-state wave functions is unlikely due to the large Li−metal distances (3.42 Å in $LiMn_2O_4$) in these spinel oxides.[40] The large shifts and hyperfine coupling constants are attributed to transfer of unpaired electron spin density from the transition-metal cations to the ^{7}Li nuclei via the interleaving oxygen anion (i.e., supertransferred hyperfine interaction). The total STH field arises from the individual contributions of the 12 nearest-neighboring B-site magnetic cations in the spinel lattice.

The hyperfine field at the A-site Li in the chemically delithiated λ-MnO_2 arises from the 12 nearest-neighboring manganese (B-site) which have a nominal +4 oxidation state. The positive shift and value of $A/\hbar$ clearly establishes a transfer of spin density to the ^{7}Li nucleus which is aligned with the static magnetic field. The STH coupling constant in $LiMn_2O_4$ is much smaller by comparison. The hyperfine interaction in this sample should be regarded as that resulting from an average Mn oxidation state of +3.5 where the Mn^{3+} and Mn^{4+} ions are indistinguishable on the NMR time scale (10^{-6} s) due to the rapid electron hopping between ions (10^{-12} s). The larger $A/\hbar$ obtained for λ-MnO_2 suggests a greater covalency in the $Li-O-Mn^{4+}$ bond than the $Li-O-Mn^{3.5+}$ bond. An increase in the nominal manganese oxidation state from +3.5 to +4 should result in a greater covalence due to the removal of the σ antibonding e electrons associated with the manganese 3d states. These observations are in qualitative agreement with the large covalence calculated for octahedrally coordinated Mn^{4+}.[41,42]

The progressive increase in the average manganese oxidation state upon substitution of the B-site manganese by lithium also results in a larger STH coupling constant in these oxides relative to the parent $LiMn_2O_4$ compound. Only Mn^{4+} is present in the $Li_4Mn_5O_{12}$ (i.e., $Li_{1.33}Mn_{1.67}O_4$) spinel oxide. The STH results from transmission of Mn^{4+}(B) unpaired electron density to ^{7}Li which reside on both A and B sites of the spinel lattice. Typically STH interactions transmitted from B-site cations to B-site cations are considered to be smaller than transmission from B-site to A-site ions. This results from the 90° B−O−B bond angle in contrast to the 125° A−O−B bond angle in spinels. However, since the ^{7}Li spectra are single Gaussian-shaped resonances, it is difficult to separately assess the STH at A- and B-site ^{7}Li nuclei. The intermediary lithium-substituted sample, $Li_{1.1}Mn_{1.9}O_4$, shows a STH coupling constant intermediate in size to those for $LiMn_2O_4$ and $Li_4Mn_5O_{12}$. Again, as in the λ-MnO_2, the progressive replacement of Mn^{3+} by Mn^{4+} results in a larger hyperfine interaction at the ^{7}Li nucleus in contrast with $LiMn_2O_4$, consistent with the removal of antibonding e electrons associated with Mn^{3+}.

The results presented in Figure 8 clearly reveal that the gradual substitution of manganese by either cobalt or nickel ions results in a significant increase in the STH coupling constant. The rate of increase in the STH is markedly larger than that for the lithium-substituted samples. This observation suggests that the cobalt ions themselves must impart a larger electron spin density through the metal−oxygen−lithium bond in addition to the increasing presence of Mn^{4+}. Nickel substitution in these materials also results in a notable increase in the STHF at the ^{7}Li nucleus. A dramatic increase in the coupling constant arises between $LiMn_{1.75}Ni_{0.25}O_4$ and $LiMn_{1.67}Ni_{0.33}O_4$ oxides. It is not clear why there is such a dramatic increase in the STH coupling constant for the $LiMn_{1.67}Ni_{0.33}O_4$ spinel. Yet the data qualitatively suggest that the presence of either nickel or cobalt in addition to Mn^{4+} conveys a greater covalence in these materials.

Conclusions

The ^{7}Li NMR shift in $LiMn_2O_4$-type spinels follows the Curie−Weiss behavior of the bulk magnetic susceptibility. The shift can be deconvoluted into temperature-dependent and -independent components. Contributions from van Vleck and diamagnetic susceptibilities may contribute to the temperature-independent component of the shift. The progressive increase in average nominal manganese oxidation state from +3.5 to +4 results in an increase in the supertransferred hyperfine field at the ^{7}Li nucleus in lithium-substituted samples. Replacement of manganese by either cobalt or nickel also results in a larger STH field at ^{7}Li nuclei in these spinel oxides. The increase in STH field for the substituted samples may arise from a greater covalence in these materials relative to the parent $LiMn_2O_4$ spinel oxide. Our results suggest that covalent or metallic bonding plays a significant role in supressing the Jahn−Teller deformation in the spinel lattice of substituted $LiMn_2O_4$ materials. Correlation of the NMR results with electrochemical cycling experiments and subsequent powder X-ray diffraction analyses of materials will be useful in further elucidating the relationship between the bonding and electrochemical properties of these materials.

Acknowledgment. We thank Marca Doeff for kindly providing the $Li_4Mn_5O_{12}$ spinel oxide sample. We are also grateful to the laboratory of Dr. Angelica Stacy (Chemistry Department, UC Berkeley) for use of their SQUID magnetometer and X-ray powder diffractometer. This work was supported by the Director, Office of Basic Energy Sciences, Chemical Sciences Division of the U.S. Department of Energy, under Contract DE-AC03-76SF00098.

References and Notes

(1) Goodenough, J. B.; Thackeray, M. M.; David, W. I. F.; Bruce, P. G. *Rev. Chim. Miner.* **1984**, *21*, 435.
(2) Thackeray, M. M. *J. Electrochem. Soc.* **1995**, *142*, 2558.
(3) Wen, S. J.; Richardson, T. J.; Ma, L.; Striebel, K. A.; Ross, Jr., P. N.; Cairns, E. J. *J. Electrochem. Soc.* **1996**, *143*, L136.
(4) Masquelier, C.; Tabuchi, M.; Ado, K.; Kanno, R.; Kobayashi, Y.; Make, Y.; Nakamura, O.; Goodenough, J. B. *J. Solid State Chem.* **1996**, *123*, 255.
(5) Voigt, J. A.; Boyle, T. J.; Doughty, D. H.; Hernandez, B. A.; Johnson, B. J.; Levy, S. C.; Tafoya, C. J.; Rosay, M. *Mater. Res. Soc. Symp. Proc.* **1995**, *393*, 101.
(6) Pistoia, G.; Wang, G.; Wang, C. *Solid State Ionics* **1992**, *58*, 285.
(7) Zhong, Q.; Bonakdarpour, A.; Zhang, M.; Gao, Y.; Dahn, J. R. *J. Electrochem. Soc.* **1997**, *144*, 205.
(8) Amine, K.; Tukamoto, H.; Yasuda, H.; Fujita, Y. *J. Electrochem. Soc.* **1996**, *143*, 1607.
(9) Cox, P. A. *The Electronic Structure and Chemistry of Solids*; Oxford University Press: Oxford, 1987.
(10) Kanzaki, Y.; Taniguchi, A.; Abe, M. *J. Electrochem. Soc.* **1991**, *138*, 333.
(11) Kumagai, N.; Fujiwara, T.; Tanno, K.; Horaba, T. *J. Electrochem. Soc.* **1996**, *143*, 1007.
(12) Mustarelli, P.; Massarotti, V.; Bini, M.; Capsoni, D. *Phys. Rev. B* **1997**, *55*, 12018.
(13) Morgan, K. R.; Collier, S.; Burns, G.; Ooi, K. *J. Chem. Soc., Chem. Commun.* **1994**, *2*, 1719.
(14) Oyang, B.; Greenbaum, S. G.; den Boer, M.; Massucco, A.; McLin, M.; Shi, J.; Fauteux, D. *Mater. Res. Soc. Symp. Proc.* **1995**, *369*, 29.

(15) Sugiyama, J.; Atsumi, T.; Koiwai, A.; Sasaki, T.; Hioki, T.; Noda, S.; Kamegashira, N. *J. Phys.: Condens. Matter* **1997**, *9*, 1729.

(16) Sugiyama, J.; Hioki, T.; Noda, S.; Kontani, M. *J. Phys. Soc. Jpn.* **1997**, *66*, 1187.

(17) Horne, C. R., to be published.

(18) Rance, M.; Byrd, R. A. *J. Magn. Reson.* **1983**, *52*, 221.

(19) Massarotti, V.; Capsoni, D.; Bini, M.; Chiodelli, G.; Azzoni, C. B.; Mozzati, M. C.; Paleari, A. *J. Solid State Chem.* **1997**, *131*, 94.

(20) Blasse, G. *J. Phys. Chem. Solids* **1966**, *27*, 383.

(21) Yamada, A., Tanaka, M. *Mater. Res. Bull.* **1995**, *30*, 715.

(22) Müller-Warmuth, W. In *Structure, Bonding, Dynamics: NMR Studies in Progress in Intercalation Research*; Müller-Warmuth, W., Schöllhorn, R., Eds.; Kluwer Academic Publishers: Dordrecht, 1994; p 435.

(23) McConnell, H. M.; Robertson, R. E. *J. Chem. Phys.* **1958**, *29*, 1361. Ibers, J.; Holm, C. H.; Adams, C. R. *Phys. Rev.* **1961**, *121*, 1620. X-ray powder diffraction data of the spinels studied confirm that the transition-metal cations are octahedrally coordinated by the oxygen anions, which should result in a symmetric **g** tensor. Therefore, the total resonance shift should not contain a contribution for the pseudocontact term.

(24) Kittel, C. *Introduction to Solid State Physics*; Wiley and Sons: New York, **1986**.

(25) Drago, R. S. *Physical Methods for Chemists*; Harcourt Brace Jovanovich: New York, 1992.

(26) Adler, S.; Reimer, J. A. *Solid State Ionics* **1996**, *91*, 175.

(27) Fishman, A. Y.; Kovtun, N. M.; Mitrofanov, V. Y.; Prokopenko, V. K.; Shemyakov, A. A. *Phys. Status Solidi B* **1989**, *156*, 597.

(28) Asai, K.; Okada, T.; Yamakaya, T.; Sekizawa, H. *Phys. Rev. B* **1988**, *37*, 9140.

(29) Geschwind, S. In *Hyperfine Interactions*;Freeman, A. J., Frankel, R. B., Eds.; Academic Press: New York, 1967.

(30) Huang, N. L.; Orback, R.; Simnek, E.; Owen, J.; Taylor, D. R. *Phys. Rev.* **1967**, *156*, 383.

(31) Simánek, E.; Sroubek, Z. In *Electron Paramagnetic Resonance*; Geschwind, S., Ed.; Plenum: New York, 1972.

(32) van Vleck, J. H. *The Theory of Electric and Magnetic Susceptibilities*; Oxford University Press: London, 1932.

(33) Jolly, W. L. *The Synthesis and Characterization of Inorganic Compounds*; Waveland Press: Prospect Heights, 1991.

(34) Freeman, A. J.; Watson, R. E. In *Hyperfine Interactions in Magnetic Materials*; Rado, G. T., Suhl, H., Eds.; Academic Press: New York, 1965; Vol. IIA.

(35) Prigge, C.; Müller-Warmuth, W.; Schöllhorn, R. *Z. Phys. Chem.* **1995**, *189*, 153.

(36) Goodenough, J. B.; Manthiram, A.; Wnetrzewski, B. *J. Power Sources* **1993**, *43*−*44*, 269.

(37) Goodenough, J. B.; Manthiram, A.; James, A. C. W. P. *Mater. Res. Soc. Symp. Proc.* **1989**, *135*, 391.

(38) Goodenough, J. B. *Proc. Symp. Maganese Dioxide Electrodes* **1985**, *85*−*4*, 77.

(39) Rao, C. N. R.; Subba Rao, G. V. *Phys. Status Solidi (Applied)* **1970**, *1*, 597.

(40) Fong, C.; Kennedy, B. J.; Elcombe, M. M. *Z. Kristallogr.* **1994**, *209*, 941.

(41) Sherman, D. M. *Am. Mineral.* **1984**, *69*, 788.

(42) Burns, R. G.; Burns, V. M. *Proc. Symp. on Manganese Dioxide Electrodes* **1985**, 85.

(43) Liu, W.; Kowal, K.; Farrington, G. C. *J. Electrochem. Soc.* **1996**, *143*, 3590.